THE JOURNAL OF BIOLOGICAL CHEMISTRY VOL. 287, NO. 26, pp. 22341–22353, June 22, 2012

Specific Serine-Proline Phosphorylation and Glycogen Synthase Kinase 3β-directed Subcellular Targeting of Stathmin 3/Sclip in Neurons*[S]

Received for publication, January 18, 2012, and in revised form, April 20, 2012 Published, JBC Papers in Press, May 10, 2012, DOI 10.1074/jbc.M112.344044

Sara Devaux, Fabienne E. Poulain[1], Véronique Devignot, Sylvie Lachkar, Theano Irinopoulou, and André Sobel[2]

From the INSERM U839, Paris F-75005, France, the Université Pierre et Marie Curie-Paris 6, UMR S839, Paris F-75005, France, and the Institut du Fer à Moulin, Paris F-75005, France

Background: Stathmins are involved in the control of neuronal differentiation.
Results: Stathmin 3 displays specific phosphorylation patterns by ERK2 and CDK5 and is a unique stathmin substrate for glycogen synthase kinase 3β mostly at neurite tips.
Conclusion: Stathmin proteins can be specifically and locally regulated by proline-directed phosphorylation.
Significance: Molecular and subcellular regulation of stathmins may contribute to the control of the development and plasticity of the nervous system.

During nervous system development, neuronal growth, migration, and functional morphogenesis rely on the appropriate control of the subcellular cytoskeleton including microtubule dynamics. Stathmin family proteins play major roles during the various stages of neuronal differentiation, including axonal growth and branching, or dendritic development. We have shown previously that stathmins 2 (SCG10) and 3 (SCLIP) fulfill distinct, independent and complementary regulatory roles in axonal morphogenesis. Although the two proteins have been proposed to display the four conserved phosphorylation sites originally identified in stathmin 1, we show here that they possess distinct phosphorylation sites within their specific proline-rich domains (PRDs) that are differentially regulated by phosphorylation by proline-directed kinases involved in the control of neuronal differentiation. ERK2 or CDK5 phosphorylate the two proteins but with different site specificities. We also show for the first time that, unlike stathmin 2, stathmin 3 is a substrate for glycogen synthase kinase (GSK) 3β both *in vitro* and *in vivo*. Interestingly, stathmin 3 phosphorylated at its GSK-3β target site displays a specific subcellular localization at neuritic tips and within the actin-rich peripheral zone of the growth cone of differentiating hippocampal neurons in culture. Finally, pharmacological inhibition of GSK-3β induces a redistribution of stathmin 3, but not stathmin 2, from the periphery toward the Golgi region of neurons. Stathmin proteins can thus be either regulated locally or locally targeted by specific phosphorylation, each phosphoprotein of the stathmin family fulfilling distinct and specific roles in the control of neuronal differentiation.

During development and plasticity of the nervous system, neuronal growth, migration, and functional morphogenesis are controlled by numerous extracellular signals and the resulting activation of intracellular signaling pathways. Many of them target directly or indirectly the subcellular cytoskeleton, including microtubules whose dynamics are essential for many cellular processes such as neuritic growth, branching, and guidance.

Among the numerous proteins involved in the control of microtubule dynamics, stathmin family proteins have been originally identified for their likely roles as relay and integrating phosphoproteins within intracellular signaling networks (1–3). They include the generic member of the family, stathmin (or stathmin 1/St1), and the products of three other genes, SCG10 (stathmin 2/St2), SCLIP (stathmin 3/St3), and RB3 (stathmin 4/St4), which possess specific N-terminal subcellular targeting sequences and a conserved C-terminal stathmin-like domain (SLD)[3] (2, 4–6). Stathmin 1 displays four well characterized phosphorylation sites by kinases such as PKA, CaM kinases, or PAK for serines 16 and 63, or ERKs and CDKs for serines 25 and 38 (7–11). The combinatorial phosphorylation of these sites, several of which are at least partially conserved in the other members of the stathmin family (2, 5), has been proposed to "relay" intracellular signals by regulating the interaction of stathmins with downstream targets (1, 3). The best known interacting partner of stathmins is tubulin, which binds their stathmin-like domains to form a 2:1 tubulin-stathmin complex, whose stability varies among stathmin family members and is strongly reduced upon their phosphorylation (12–18). Stathmins can thus sequester free tubulin that may result in inhibiting microtubule growth and/or promoting microtubule collapse (2, 12, 19). Upon phosphorylation, they may release previously bound tubulin and hence promote microtubule growth (20). This combined property designates stathmins as key players in the control of microtubule dynamics, a function

* This work was supported by the Institut National de la Santé et de la Recherche Médicale (INSERM), Université Pierre et Marie Curie (UPMC), and the Agence Nationale pour la Recherche (ANR).
[S] This article contains supplemental Fig. S1.
[1] Present address: Dept. of Neurobiology and Anatomy, University of Utah, Salt Lake City, UT.
[2] To whom correspondence should be addressed: UMR-S 839 INSERM/UPMC, and the Institut du Fer à Moulin,17 rue du Fer à Moulin, 75005 Paris, France. Tel.: 33-1-45-87-61-42; Fax: 33-1-45-87-61-32; E-mail: andre.sobel@inserm.fr.

[3] The abbreviations used are: SLD, stathmin-like domain; PRD, proline-rich domain; DCX, doublecortin; GSK-3β, glycogen synthase kinase 3β.

that stathmins 2–4 can achieve locally, at the Golgi or intracellular vesicles, thanks to their palmitoylation regulated membrane anchoring domain (5, 14, 21–24). In neurons, stathmins bearing vesicles are present within neuritic extensions and concentrated at their tips, together with dynamic microtubules in the central domain of axonal growth cones (20, 23, 25, 26).

Stathmins have been suggested to play a role in the control of diverse stages of neuronal differentiation, including neuronal polarity, axonal growth and branching, or dendritic development (2, 20, 26–30). They are essentially expressed in the nervous system during embryonic and postnatal development with, however, at least partially distinct expression profiles for the various members of the family, suggesting distinct functions in the control of neural patterning and morphogenesis (2, 5, 6, 31, 32). Although stathmins 2 and 3 display identical expression and subcellular localization in hippocampal neurons in culture, RNAi inhibition of stathmin 2 or 3 expression results in growth cone expansion or increased axonal branching, respectively (26). Also, inhibition of stathmin 3 expression in Purkinje cells of cerebellar slices in culture impairs the formation of the dendritic tree (27), indicating that the major role of any given stathmin may depend on its specific, local, and temporal subcellular and cellular environment.

An important issue is thus deciphering specificities among the various members of the stathmin family, their roles, and the underlying molecular and regulatory features (2, 13). Within their highly similar SLDs, stathmins possess a short divergent proline-rich domain (PRD) (6), linking their tubulin binding cap with their duplicate tubulin-binding regions (16, 33). In stathmins 1–3, this region is flanked by two proline-serine phosphorylation sites that have been shown for stathmins 1 and 2 to be targets for proline-directed kinases such as ERKs and CDKs (7, 34). The phosphorylation of stathmin 3 has, however, not been previously characterized. We hypothesized that functional differences between stathmins 2 and 3 might be due in part to differences in their regulation by phosphorylation (20, 26). We reveal here at least one additional phosphorylation site within the PRD of stathmin 3 and show that stathmins 2 and 3 are phosphorylated differently by proline-directed kinases involved in the control of neuronal differentiation. ERK2 and CDK5 display different site specificities on the two proteins. Furthermore, we show for the first time that stathmin 3, unlike stathmin 2, is a substrate for GSK-3β, a proline-directed kinase involved in the control of neuronal morphogenesis (35–39), which phosphorylates a serine residue within its PRD. Finally, we reveal a specific subcellular localization of GSK-3β-phosphorylated stathmin 3 at neuritic tips and within the actin-rich peripheral zone of the axonal growth cone of differentiating hippocampal neurons in culture. Altogether, our results provide molecular clues to the specific regulation and regulatory roles of stathmin 3, and substantiate our hypothesis that each phosphoprotein of the stathmin family fulfils distinct and specific roles in the control of neuronal differentiation.

EXPERIMENTAL PROCEDURES

Plasmid Constructs and Mutations—For bacterial expression, SLD of stathmin 3 (WT and mutants) and stathmin 2 were expressed in the pET-8C vector as previously described (13). For eukaryote expression, St3-myc and mutants were expressed in the pcDNA3-myc vector as previously described (40). Mutations to alanines of serines 60, 68, or 73 of St3-SLD were generated by site-directed mutagenesis using the QuikChange mutagenesis kit (Stratagene) with pairs of complementary mutagenic primers. All constructs were confirmed by DNA sequencing.

Protein Expression and Purification—Recombinant SLD expressions were performed as previously described (13). Briefly, plasmids encoding the respective SLDs were used to transform the *Escherichia coli* BL-21 (Stratagene). An overnight preculture, grown at 37 °C, was used to seed 100 ml of LB medium. At exponential phase, recombinant protein expression was induced for 3 h by adding 0.4 mM isopropyl thio-β-D-galactoside. Cells were then pelleted by centrifugation, resuspended in 20 mM Tris-HCl, 1 mM EGTA, pH 8.0, containing Complete antiprotease mixture (Roche Diagnostics) and heated to 100 °C for 15 min. The pellets were sonicated three times for 1 min on ice before ultracentrifugation at 100,000 $\times$ *g* (Optima MAX ultracentrifuge, rotor TLA 100.2, Beckman Instruments) for 6 min at 4 °C to yield the S2 supernatants and P2 pellets. S2 supernatants were loaded on a Q-Sepharose FF anion exchange column (GE Healthcare) and eluted with a 0–200 mM NaCl linear gradient in 20 mM Tris-HCl, 1 mM EGTA, pH 8.0. The eluted SLD positive fractions were pooled and concentrated with Centriprep 10 (Millipore). Protein concentrations were determined by optical density at 206 nm.

Phosphospecific Antibodies—Phosphospecific rabbit polyclonal antibodies directed to stathmin 3 phosphorylated on serine 60 (anti-St3–60P), 68 (anti-St3–68P), or 73 (anti-St3–73P) were generated using the phosphorylated synthetic KLH-conjugated peptides ILKS[PO3H2]SDLS, DLSPES[P03H2]VLSS, and VLSS[P03H2]PKRK as antigens, respectively. The specific antibodies were purified by double peptide affinity column chromatography against the immunogenic phosphorylated peptide and then the corresponding unphosphorylated peptide, and their titers were determined by ELISA (Eurogentec).

In Vitro Phosphorylation—Phosphorylation reactions with various substrates were performed in 20 μl containing 60 mM HEPES, pH 7.5, 10 mM $MgCl_2$, 20 mM DTT, 20 mM EDTA, 10% glycerol, 1 μM [γ-^{32}P]ATP (approximately 300 cpm $\times$ pmol^{-1}), 0.5 μl of protein kinase stock solution and 300 ng of substrate. The substrates used were St2-SLD, St3-SLD, St3/60A-SLD, St3/68A-SLD, and St3/73A-SLD recombinant proteins, produced, and purified as described above. Protein kinases used were CDK5/p25NCK (Invitrogen), GSK-3β (Ozyme), and ERK2/p42 MAP kinase (Ozyme). Reactions were incubated for increasing times at 30 °C, stopped with 10 μl of 3$\times$ SDS gel loading buffer (NuPAGE LDS Sample Buffer containing reducing buffer, from Invitrogen), and loaded on a 12% acrylamide SDS gel. After electrophoresis the gel was stained with Coomassie Blue, dried, and exposed in an FLA-7000 phosphorimager (Fujifilm) for radioactivity detection and quantification. Coomassie staining of relevant bands was quantified with an Odyssey Imaging System (LI-COR Biosciences) at 700 nm.

HeLa Cell Culture and Transfection—HeLa cells were grown in DMEM (Dulbecco's modified Eagle's medium)-Glutamax with 10% decomplemented fetal calf serum and 1% penicillin/

streptomycin (Invitrogen) at 37 °C in a humidified atmosphere containing 5% CO_2. Twice a week, cells were dissociated in 0.25% trypsin and 1 mM EDTA (Invitrogen), and then diluted 1:10 before replating. For transfection, HeLa cells were seeded at 12.5×10^3 cells/cm^2 in 35-mm dishes. They were transfected 16 h after plating, using the liposoluble reagent Lipofectamine™ 2000 (Invitrogen), according to the manufacturer's instructions: 3 μl of reagent and 1 μg of plasmid DNA were used for one 35-mm dish.

Primary Hippocampal Neurons—Primary cultures of hippocampal neurons from E18 Sprague-Dawley or Wistar rats were prepared as described (41). Briefly, hippocampi were dissociated by trypsinization and trituration and plated for immunofluorescence on poly-L-lysine-coated glass coverslips at 2.4×10^3 cells/cm^2 or for biochemical analysis in poly-L-lysine-coated 35-mm culture dishes at 3×10^5 cells per dish. After cells were allowed to attach for 3 h in attachment medium (10% horse serum, 2 mM L-glutamine, 1 mM sodium pyruvate, minimal essential medium (Invitrogen)), the medium was changed for Neurobasal™ (Invitrogen) supplemented with 2% B27 (Invitrogen) and 2 mM L-glutamine (Invitrogen).

Cell Extracts and Western Blot—Hippocampal neurons cultured in 35-mm dishes for 3 days were washed with cold PBS (0.15 M NaCl, 25 mM KCl, 15 mM KH_2PO_4, 64 mM $Na_2HPO_4 \cdot 12H_2O$) and lysed in 50 μl of neuron lysis buffer (10 mM Tris-HCl, pH 7.5, 2 mM EDTA, 1% SDS) containing Complete protease inhibitor (Roche Diagnostics) and phosphatase inhibitor (Thermo Scientific) mixtures. Samples were then vortexed for 10 min at 4 °C and centrifuged at 20,000 × *g* for 15 min at 4 °C. Supernatants were incubated with 1 ml of acetone and centrifuged at 20,000 × *g* for 15 min at 4 °C. Precipitated proteins were resuspended in NuPAGE LDS Sample Buffer containing reducing buffer (Invitrogen) and proteins from one culture dish were loaded and electrophoresed on a 12% polyacrylamide gel (Invitrogen). Migrated proteins were transferred to nitrocellulose membranes, which were blocked with 5% milk/TBS (25 mM Tris-HCl, pH 7.5, 3 mM KCl, 140 mM NaCl). Proteins of interest were revealed by incubation with appropriate antibodies diluted in blocking buffer: purified anti-stathmin 3 (1:500) and anti-stathmin 2 (1:500) rabbit polyclonal antibodies (26); anti-stathmin 1 (1:5,000) rabbit polyclonal antiserum (42); anti-St3–60P (1:500) and anti-St3–73P (1:500) purified rabbit polyclonal antibodies (see above); anti-phospho-Tau (Ser-199) (1:1,000) (Chemicon) and anti-α-tubulin E7 monoclonal antibodies (1:10,000). Primary antibodies were revealed with IRDye 800- or IRDye 680-conjugated secondary antibodies (1:5000) (Rockland Immunochemicals), which were visualized using the Odyssey Imaging System (LI-COR Biosciences).

Transfected HeLa cells cultured in 35-mm dishes were washed with cold PBS and lysed in 50 μl of HeLa lysis buffer (50 mM Tris-HCl, pH 7.5, 125 mM NaCl, 10% glycerol, 1% Triton X-100) containing Complete protease inhibitor (Roche Diagnostics) and phosphatase inhibitor (Thermo Scientific) mixtures. The rest of the protocol was identical to that for hippocampal neurons except that only ½ of proteins per culture dish were loaded for polyacrylamide gel electrophoresis.

Drug Treatments and Immunofluorescence—Hippocampal neurons were treated with 10 or 20 μM GSK-3β inhibitor AR-A014418/Inhibitor VIII (Merck) or with 5 or 10 μM inhibitor XV (SB216763) (EMD) for 3 or 24 h. Neurons were fixed at 37 °C with 4% paraformaldehyde in 0.2 M phosphate buffer (150 mM Na_2HPO_4, 50 mM NaH_2PO_4) for 5 min and with renewed 4% paraformaldehyde solution for 10 min. They were then permeabilized with 0.1% Triton X-100 for 6 min and blocked for 1 h with 3% BSA in TBS (25 mM Tris-HCl, pH 7.5, 3 mM KCl, 140 mM NaCl). The cells were then incubated overnight at 4 °C with the appropriate primary antibodies in blocking buffer: purified rabbit polyclonal anti-stathmin 3 and 2 (1:500), anti-St3–60P (1:500), and anti-St3–73P (1:500), and mouse monoclonal anti-tyrosinated tubulin (1:10,000). After 5 washes with TBS, they were incubated with Alexa 488-conjugated anti-rabbit IgG antibody (Invitrogen) or Cy3-conjugated anti-mouse IgG (Jackson) that was diluted 1:500 in blocking buffer. For triple labeling including actin, cells were incubated with Alexa 546-phalloidin (Molecular Probes) that was diluted 1:1,000 in TBS for 1 h after the secondary antibody incubation. For triple labeling including Golgi, cells were incubated with anti-CTR 433 (1:10) (gift from M. Bornens, Institut Curie, Paris) overnight, washed 5 times, and incubated again with Cy5-conjugated anti-mouse IgG (1:500) (Jackson) before tubulin and stathmin 3 or stathmin 2 labeling. Cells were finally rinsed extensively in TBS and then mounted in a Mowiol solution.

Immunofluorescence Microscopy and Image Analysis—Images were acquired with a ×40 objective mounted on a LEICA DM 6000 microscope (Leica Microsystems), equipped with a Micromax camera (Roper Scientific) controlled with Metamorph (Universal Imaging) or a LEICA SP2 confocal laser scanning microscope and a ×63 objective (Leica microsystems). Neurons showing a healthy morphology based on tubulin labeling were chosen randomly on each slide. All acquisition features were kept constant for the whole study. Image names were randomized for blind analysis.

Stathmin 2 and stathmin 3 labeling intensities were quantified in the Golgi and the rest of the cytoplasm automatically, using Metamorph software and a home written journal. Tubulin and Golgi (CTR 433)-labeled images were segmented to obtain the cytoplasm and Golgi areas. The cytoplasm area with the exclusion of the Golgi was obtained by logical operations on the above defined areas. Stathmin 2 and 3 average intensities in the Golgi and cytoplasm excluding the Golgi were computed for each cell, from which the ratio between the average intensity in the Golgi and the rest of the cytoplasm was deduced. Quantification was made on 20 cells in three different experiments. Histograms presented in Fig. 7 correspond to the mean of this ratio for one representative experiment. Analysis was performed using Metamorph, Microsoft Excel, and GraphPad Prism5. All statistical comparisons of immunofluorescence intensities were made using the Mann-Whitney test. Images were prepared for printing using Adobe Photoshop.

RESULTS

Stathmins Possess Variable PRDs with Specific Serine-Proline Potential Phosphorylation Sites—Despite their high degree of sequence identity and similar expression and localization in

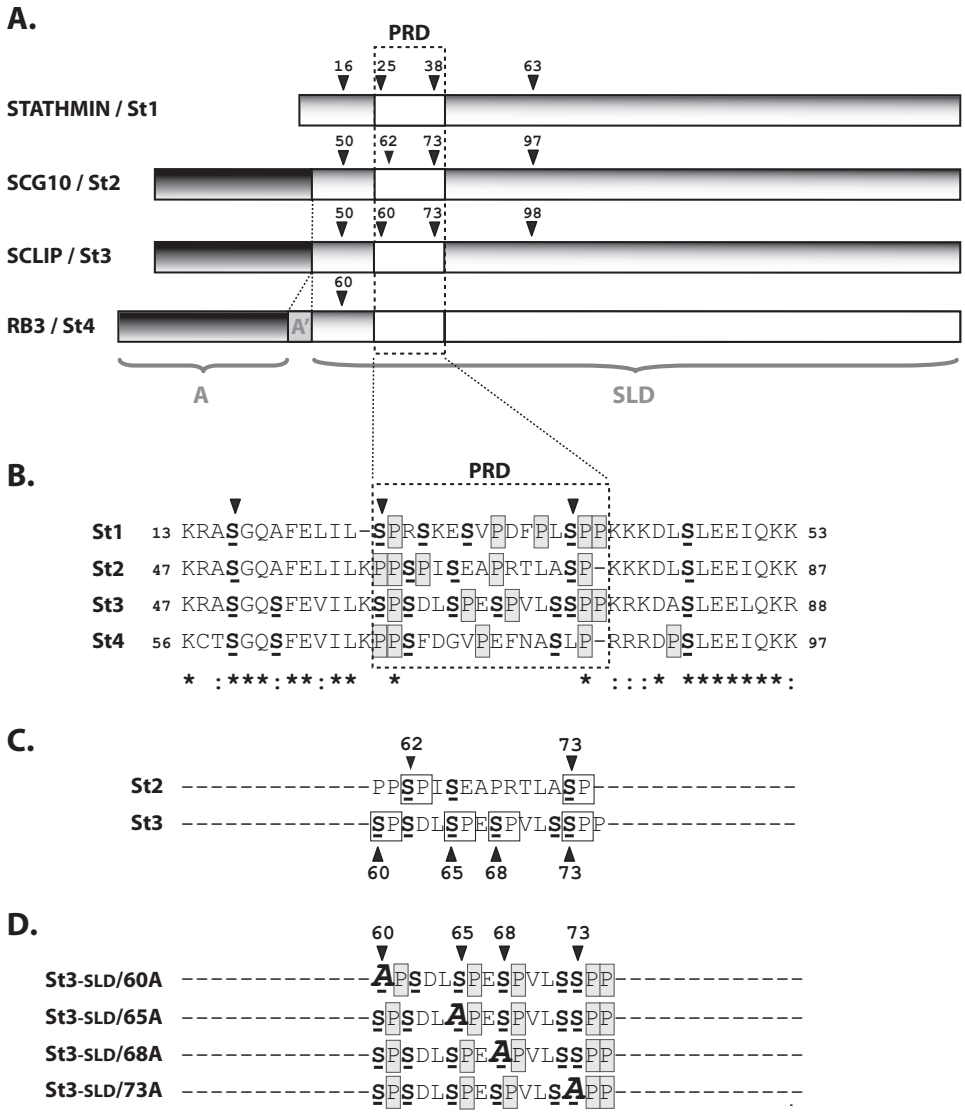

FIGURE 1. **The stathmin family, the PRD domain and mutants used in this study.** *A,* schematic representation of the stathmin family proteins. Stathmins 1–4 possess a 65–75% conserved SLD with an internal divergent PRD (*broken box*). Stathmins 2–4 possess an additional subcellular targeting domain A (and *A′* for stathmin 4). The four phosphorylation sites identified experimentally in stathmins 1 and 2 are indicated, as well as the corresponding, homologous sites on stathmins 3 and 4 (*arrowheads*). *B,* amino acid alignment of the PRD (*broken box*) and surrounding sequence of the four mouse stathmins. Amino acid identities (*stars*) and homologies (*columns*) are indicated in the *bottom line*, clearly revealing the divergence among stathmins within their PRD, although the PRD of each stathmin is well conserved through evolution (see supplemental Fig. S1). Serines are *bold underlined*, and prolines are *boxed*, highlighting the high proline content of the PRD. *C,* comparison of the PRDs of stathmins 2 and 3, showing (*boxes*) the serine-proline phosphorylation sites identified in stathmin 2, and the homologous (serines 60, 73) as well as additional (serines 65, 68) serine-proline sites within stathmin 3. *D,* schematic representation of PRD mutants of stathmin 3-SLD used in this study. In each mutant, one of the serines within a serine-proline site is replaced by an alanine.

hippocampal neurons in culture, RNAi invalidation revealed very different and specific roles for stathmin 2 and 3 in axon morphogenesis (26). Although they have been proposed to display the characteristic four conserved phosphorylation sites originally identified in stathmin 1 (5–7, 34), we reasoned that differences in their roles and regulation might result from differences in their phosphorylation. We therefore re-examined their amino acid sequences with an emphasis on differences instead of identities (Fig. 1 and supplemental Fig. S1). The overall highly conserved stathmin-like SLD domain of all four stathmins in vertebrates includes a short diverging proline-rich stretch of amino acids (PRD) (2, 4–6) (Fig. 1*B*). Indeed, although the PRD of each stathmin is highly conserved through evolution in vertebrates (supplemental Fig. S1), its sequence is characteristic of the corresponding member of the stathmin family. In stathmin 1, this region (residues 25–40) is bordered by two serine-proline phosphorylation sites (serines 25 and 38) that are substrates for ERK2 and CDK kinases, two kinase families known to be involved in the control of neural differentiation (43, 44), with a preference of serine 25 for ERKs and 38 for CDKs (7, 9). The PRD of stathmin 2 (residues 59–74) harbors corresponding serine-proline sites at positions 62 and 73 that are also substrates for the same kinases, with a more exclusive specificity of CDKs for serine 73 (34). The phosphorylation of stathmin 3 had not been characterized so far. Its PRD (residues 59–75) also displays corresponding serine-prolines at flanking positions 60 and 73, but also two addi-

tional ones, at positions 65 and 68 (Fig. 1*C*), which may be additional phosphorylation sites for regulating the functions of stathmin 3.

Specific Phosphorylation of Stathmin 3 by CDK5, ERK2, and GSK-3β in Vitro—We therefore decided to examine and characterize the phosphorylation of stathmin 3 by three classical serine-proline-directed protein kinases involved in signaling in the nervous system, namely ERK2, CDK5, a neuronal CDK previously shown to phosphorylate stathmin 1 (45), and GSK-3β, a serine-proline directed kinase involved in axon formation and branching (35–39) and neurogenesis (37, 46), and not previously reported to phosphorylate stathmin proteins.

We first compared the phosphorylation of recombinant SLDs of stathmins 2 and 3 *in vitro* in the presence of γ-[^{32}P]ATP and the respective kinases (Fig. 2*A*). As revealed by SDS-PAGE analysis of [^{32}P]phosphate incorporated in each of the proteins, ERK2 and CDK5 promoted the phosphorylation of the SLDs of both stathmins 2 and 3 to similar levels, although ERK2 was somewhat more efficient to phosphorylate stathmin 2. Remarkably, stathmin 3 appeared to be a substrate also for GSK-3β, whereas this kinase did not promote any detectable phosphate incorporation into stathmin 2.

To identify the stathmin 3 site(s) phosphorylated by each of the three proline-directed kinases tested, we generated St3-SLD single alanine mutants of the two flanking serines 60 and 73, and of the two specific stathmin 3 PRD serines 65 and 68 (Fig. 1*D*), and probed them for *in vitro* phosphorylation kinetics (0–120 min) in comparison with the wild type (WT) protein (Fig. 2, *B* and *C*). Alanine mutation of serine 60 did not inhibit phosphorylation of St3-SLD by CDK5 or ERK2, but it did inhibit phosphorylation by GSK-3β by at least 70%. On the other hand, mutation of serine 73 did not inhibit phosphorylation by ERK2 but did inhibit phosphorylation by CDK5 by about 50%. Among the two additional serine-proline sites in stathmin 3, mutation of serine 65 did not inhibit phosphorylation by any of the three kinases tested (not shown), whereas mutation of serine 68 inhibited phosphorylation of St3-SLD by both CDK5 (~40% inhibition) and ERK2 (~80% inhibition). Altogether, these results indicate that CDK5 phosphorylates similarly serines 68 and 73, whereas ERK2 targets mostly serine 68 and GSK-3β mostly serine 60. These results show that phosphorylation of stathmin 3 by the three proline-directed kinases tested is indeed specific, differing from sites predicted by homology with the previously described phosphorylation sites of stathmins 1 and 2 (serine 73 for CDKs and serines 60 and to a lesser extent 73 for ERK2). Altogether, our *in vitro* phosphorylation results unravel novel kinase specificities and phosphorylation sites unique to stathmin 3 among stathmin proteins, and likely contributing to its specific biological regulation and properties.

Antiphosphostathmin 3 Antibodies Reveal in Vitro and in Vivo Phosphorylation of Stathmin 3 at Serines 60 and 73—To further characterize the phosphorylation of stathmin 3 *in vitro* and *in vivo*, we immunized rabbits with peptides including the phosphorylated forms of the previously characterized phosphorylation sites of stathmin 3 at serines 60, 68, and 73. Whereas the ELISA titer of the antiserum directed to phosphoserine 68 was unfortunately too low, we obtained potent and specific purified polyclonal antibodies directed to phosphoserines 60 (anti-St3–60P) and 73 (anti-St3–73P), as revealed by ELISA and cross-specific phosphopeptide dot blots (not shown). To further characterize their specificity for the phosphorylated residues within the entire SLD of stathmin 3, we expressed various myc-tagged St3-SLD forms, either wild type (WT) or mutated to alanine in positions 60 (St3/60A) or 73 (St3/73A) in HeLa cells, to allow their phosphorylation by endogenous kinases. The corresponding cell extracts were analyzed by Western blotting with monoclonal anti-myc for total transfected protein expression, and with purified anti-St3–60P and anti-St3–73P antibodies to evaluate their phosphorylation on the corresponding sites (Fig. 3*A*). As expected, whereas all three proteins were expressed to similar levels (anti-myc labeling), anti-St3–60P recognized the WT protein and St3/73A, but not St3/60A. Conversely, anti-St3–73P recognized the WT protein and St3/60A but not St3/73A. The two antibodies are hence efficient to recognize the whole protein in its phosphorylated states, and fully specific for their target phosphosites.

The specific antibodies were then used to identify directly the sites phosphorylated by the three proline-directed kinases, whose target sites were inferred from recombinant mutation in our *in vitro* phosphorylation studies. Recombinant St3-SLD was phosphorylated *in vitro* in the presence of GSK-3β, CDK5, or ERK2 as above but with only trace amounts of radioactive γ-[^{32}P]ATP to control for actual phosphate incorporation. The control and phosphorylated proteins were then analyzed by Western blot with anti-St3, anti-St3–60P, and anti-St3–73P purified antibodies (Fig. 3*B*). As a further control for the phosphospecificity of our novel antibodies, unphosphorylated stathmin 3 was as expected not recognized by the phosphostathmin 3-directed antibodies. Anti-St3–60P recognized St3-SLD phosphorylated in the presence of GSK-3β and, to a lesser extent, ERK2, whereas anti-St3–73P recognized only the protein phosphorylated by CDK5. These results, in agreement with the *in vitro* phosphorylation assay with the various serine to alanine mutated St3-SLDs shown in Fig. 2, strongly suggest that GSK-3β phosphorylates stathmin 3 essentially at serine 60, and that this same serine could also be phosphorylated likely as a secondary site by ERK2. In contrast, CDK5 phosphorylates stathmin 3 at serine 73, which might also be poorly phosphorylated by GSK-3β.

Taking advantage of the good titer and specificity of the anti-phosphostathmin 3 antibodies, we examined endogenous phosphorylation of stathmin 3 in neurons. Western blots of extracts from hippocampal neurons in culture reveal that both anti-St3–60P and anti-St3–73P recognize a band at the level of the endogenous stathmin 3 protein revealed by the anti-stathmin 3 antibody (Fig. 3*C*). This result is a good indication that stathmin 3 phosphorylation on serines 60 and 73 occurs *in vivo.*

Stathmin 3 Phosphorylated on Serine 60 or 73 Displays Divergent Subcellular Localization during Neuronal Differentiation—We have shown previously that stathmin 3 plays essential roles in axonal morphogenesis of embryonic rat hippocampal neurons in culture (26), a powerful and widely used model for studying neuronal differentiation (47). As a member of the stathmin phosphoprotein family, stathmin 3 was predicted to be regulated by phosphorylation (5), and the detection of stath-

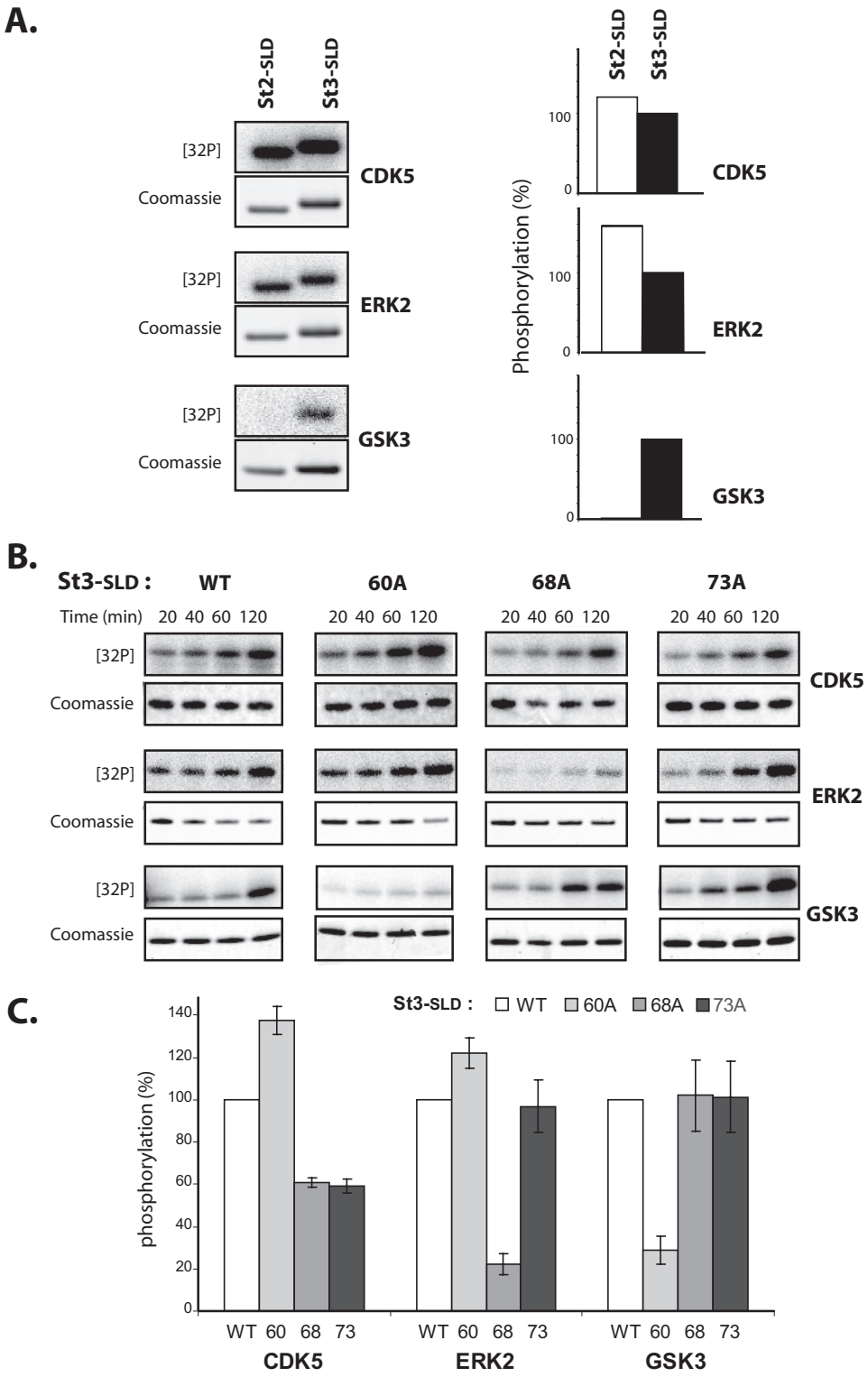

FIGURE 2. ***In vitro* phosphorylation of stathmin 3 by CDK5, ERK2 and GSK-3β.** *A,* stathmin 2 (*St2*) or 3 (*St3*) SLD recombinant proteins were phosphorylated by CDK5, ERK2, or GSK-3β for 60 min and analyzed by SDS-PAGE followed by Coomassie Blue staining and phosphorimaging for ^{32}P incorporation (*left panel*). Their relative phosphorylation by each kinase is revealed by comparing the ratio of the ^{32}P over the Coomassie Blue signals, the resulting ratio being arbitrarily set to 100% for stathmin 3 (*right panel*), revealing comparable phosphorylation of stathmins 2 and 3 by CDK5 and ERK2, as well as the unique phosphorylation of stathmin 3 by GSK-3β. *B,* wild type (*WT*) stathmin 3 SLD recombinant protein and its alanine mutated forms (see Fig. 1) at the indicated serine residues were phosphorylated by CDK5, ERK2, or GSK-3β for the indicated times. Reaction products were analyzed by SDS-PAGE followed by Coomassie Blue staining and phosphorimaging for ^{32}P incorporation. *C,* the ratio of the ^{32}P incorporated at 60 min over the Coomassie Blue signal from at least three independent experiments such as in *B* was quantified, the resulting value being arbitrarily set at 100% for the wild type protein. Mean ± S.E.

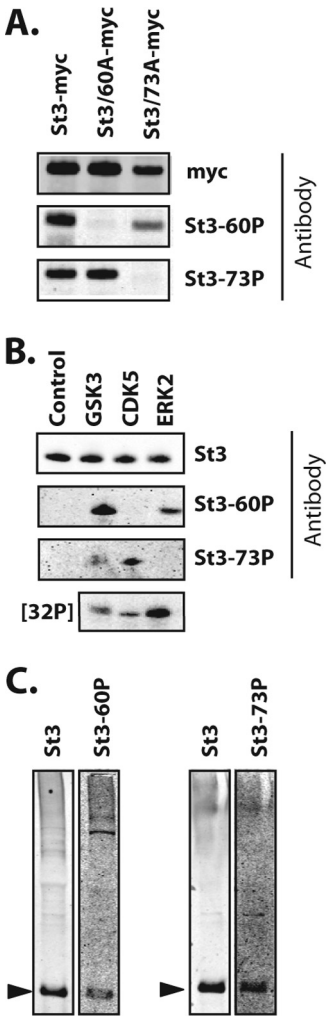

FIGURE 3. **Characterization of stathmin 3 phosphospecific antibodies.** *A*, extracts from HeLa cells transfected with various stathmin 3 constructs (*St3-myc*, *St3/60A-myc*, and *St3/73A-myc*) were analyzed by Western blot using anti-myc for total and the indicated stathmin 3 phosphospecific antibodies, demonstrating their actual specificities for the corresponding phosphorylation sites. *B*, recombinant WT St3-SLD protein was phosphorylated *in vitro* by GSK-3β, CDK5, or ERK2, respectively, using cold (*upper panels*) or radioactive ATP (*bottom panel*, [^{32}P]) in parallel experiments, and run on SDS-PAGE. The nonradioactive samples were analyzed by Western blot with the indicated antibodies for total (*St3*) and the indicated stathmin 3 phosphospecific forms, allowing the identification of the sites phosphorylated by the various kinases. The radioactive reaction products were analyzed by phosphorimaging to ascertain phosphate incorporation with each kinase tested. *C*, total extracts of hippocampal neurons in culture were analyzed by Western blot for total and phosphorylated stathmin 3 using the indicated antibodies, demonstrating the endogenous neuronal phosphorylation of stathmin 3 on serines 60 and 73.

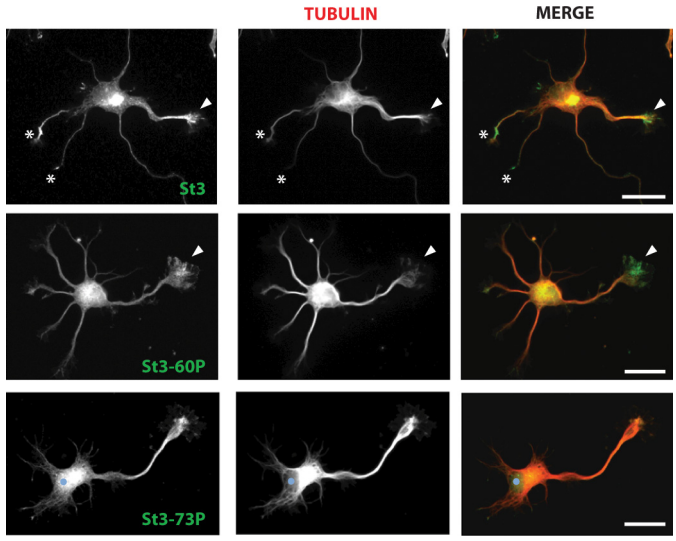

FIGURE 4. **Subcellular localization of St3–60P and St3–73P immunoreactivity during neuronal differentiation.** Hippocampal neurons in culture were immunolabeled with purified anti-stathmin 3, St3–60P, or St3–73P antibodies, together with anti-tubulin to reveal the overall shape of the cells. The accumulation of St3–60P but not St3–73P immunoreactivity at growth cones (*arrowheads*) and neurite tips (*asterisks*) is clearly visible. *Bar* = 20 μm.

min 3 phosphorylated on serines 60 and 73 in hippocampal neurons in culture (Fig. 3) indicates that this is actually the case *in vivo*. We therefore examined closely the subcellular localization of stathmin 3 phosphoforms in hippocampal neurons during their differentiation in culture.

As we have shown previously (26), stathmin 3 is essentially localized at the Golgi and vesicle-like structures throughout the cell body and along neurites, and presents a specific accumulation at the axonal growth cone of differentiating neurons (Fig. 4), as visualized by immunocytochemistry with a polyclonal antibody recognizing all, nonphosphorylated and phosphorylated forms of stathmin 3. In contrast to total stathmin 3 labeling, anti-phosphostathmin 3 antibodies revealed distinct subcellular localizations of stathmin 3 phosphorylated on serines 60 and 73, respectively. Both anti-St3–63P and anti-St3–73P revealed a diffuse labeling in the cell body, not restricted to the Golgi and often including the nuclear region, mostly in the case of St3–73P. In the growing process shafts, the two antibodies also revealed a diffuse, less punctuate and vesicle-like staining than the total stathmin 3 labeling. This diffuse and more extended labeling with the anti-phosphostathmin 3 antibodies suggests that the corresponding phosphoforms may be partially soluble and have specific local functions within the neuron. The low level of soluble labeling with the anti-stathmin 3 antibody, which also recognizes the phosphoforms, suggests that the latter, although strongly labeled by the corresponding specific antiphosphostathmin antibodies, represent a minor proportion of total stathmin 3. Interestingly, the immunostaining within the neurite tips and growth cones strongly diverged between the two phosphoforms: only anti-St3–60P displayed a labeling at neurite tips and within the peripheral, actin-rich domain of the growth cone (Figs. 4). Moreover, anti-St3–60P seemed to stain more strongly the growth cone than other neurite tips. The similar labeling with the anti-stathmin 3 and anti-St3–60P antibodies in growing lamellipodia suggests that a significant proportion of stathmin 3 is phosphorylated on serine 60 in this cellular region. In growth cone peripheral regions the anti-St3–60P labeling seems relatively more intense than the anti-stathmin 3 one, which suggests that stathmin 3 in these regions is mostly phosphorylated on serine 60. Altogether, these observations reveal for the first time distinct subcellular localizations of stathmin 3 depending on its phosphorylation at different sites, which might reflect either its specific phosphorylation at corresponding locations within the cell or relocalization of the protein according to its phosphorylation state, most likely in relationship with its functional regulation.

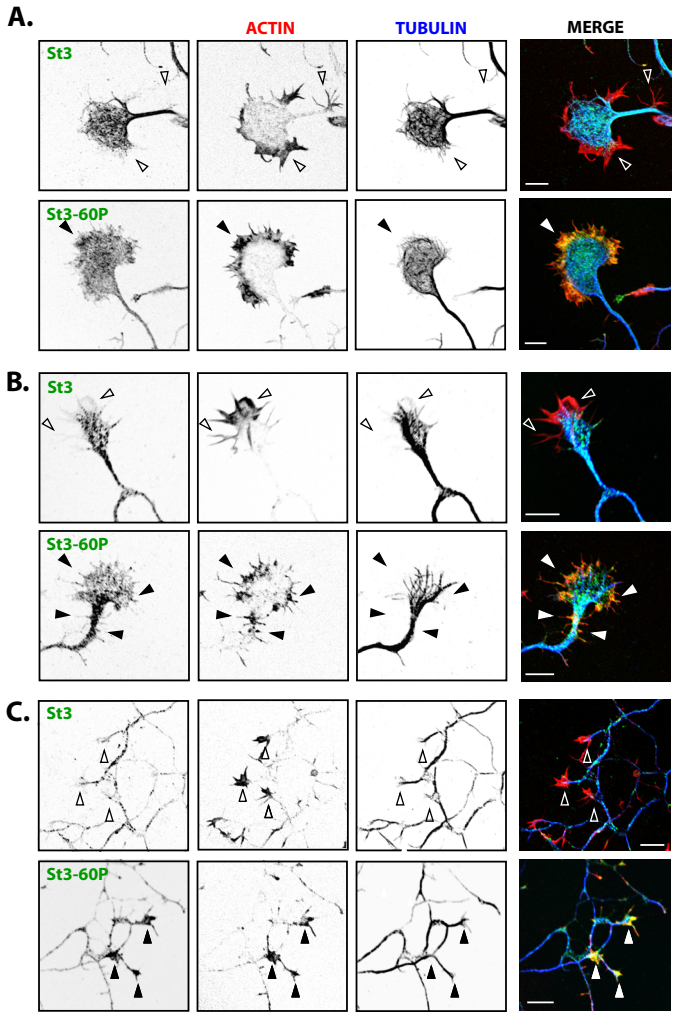

FIGURE 5. **St3–60P colocalization with actin rich domains in the growth cone and neurites.** Hippocampal neurons in culture were immunolabeled with purified anti-stathmin 3 or St3–60P antibodies (*green*), together with anti-tyrosinated tubulin (*blue*) to reveal the dynamic microtubule cytoskeleton, and with phalloidin to highlight the actin-rich regions (*red*). Examples of various actin-rich domains (*A* and *B*) at the peripheral zone of the axonal growth cone and in filopodia and (*C*) at neurite tips and forming branch sites, showing specific colocalization of St3–60P immunoreactivity (*filled arrowheads*), but no accumulation of unphosphorylated stathmin 3 (*empty arrowheads*). Confocal microscopy, *bar* = 10 μm.

Stathmin 3 Phosphorylated on Serine 60 Is Localized Partially within Actin-rich Regions of Growth Cones, Neurite Tips, and Branch Sites—The growth cone can be divided into three regions: the central domain containing splayed microtubules, the transition domain where actin filaments anchor into a loose MT network, and the peripheral domain containing a dense meshwork of actin and few exploratory microtubules (48). Because we noticed differences in St3–60P *versus* total stathmin 3 immunolabeling between the peripheral and central domains of the growth cone (Fig. 4*B*), we decided to examine more closely the localization of St3–60P in the growth cone in relationship to the cytoskeleton. We performed triple labeling of stathmin 3 or St3–60P with both actin and tubulin on hippocampal neurons after 3 days in culture (Fig. 5), a stage when growth cones are fully mature and active. As previously described (26), confocal analysis revealed that stathmin 3 is abundant in the growth cone central domain, where it partially follows the dense dynamic microtubule network, whereas it does not appear significantly colocalized with peripheral actin except along some exploratory microtubules penetrating the peripheral region (Fig. 5, *A* and *B*). Immunoreactivity of its St3–60P phosphoform is also present in the growth cone central domain, possibly at a relatively lower density than total stathmin 3. However, unlike total stathmin 3, St3–60P immunoreactivity also labels the peripheral actin-rich domain and its filopodia, as ascertained by the yellow/orange color in the corresponding merged images of Fig. 5, *A* and *B*. It is also strongly detected along actin-rich filopodial extensions stemming from the distal axon shaft (Fig. 5, *A* and *B*), as well as in other neurite tips and likely neuritic branch sites that appear also almost devoid of microtubules (Fig. 5*C*). The lack of visible labeling for total stathmin 3 in the actin-rich extending regions reveals that, although it represents a minor fraction of total stathmin 3 in neurons, the majority of stathmin 3 present in these regions is phosphorylated on serine 60.

GSK-3β Inhibitors Specifically Inhibit Phosphorylation of Stathmin 3 Serine 60 in Neurons in Vivo—We have shown that stathmin 3 can be phosphorylated *in vitro* on serine 60 by GSK-3β and that, unlike other phosphorylated forms of stathmin 3 such as St3–73P, St3–60P has a specific and particular distribution within the growth cone of differentiating hippocampal neurons in culture. To assess whether stathmin 3 is phosphorylated by GSK-3β *in vivo*, we examined the effect of pharmacological inhibition of the kinase in neurons in culture with two distinct GSK-3β-specific inhibitors: AR-A014418 (49) and inhibitor XV (50). We checked that AR-A014418 efficiently inhibited GSK-3β-mediated ^{32}P incorporation into recombinant St3-SLD in the nanomolar range *in vitro* (Fig. 6*A*). To test the efficacy of the two inhibitors on GSK-3β activity *in vivo*, we monitored the amount of phosphorylation of Tau, a well known GSK-3β substrate (51), by immunoblotting treated cell extracts with a specific antibody directed to Tau phosphorylated at serine 199. As expected, the phosphorylation of Tau decreased upon pharmacological treatment with the GSK-3β inhibitors, dose dependently in the 10 μM range *in vivo* (Fig. 6*B*). Interestingly, both AR-A014418 and inhibitor XV treatments resulted, at the same concentrations, in a decrease also of stathmin 3 phosphorylated on serine 60, as revealed by immunoblotting of the same extracts with the purified anti-St3–60P antibody (Fig. 6*C*). On the other hand, no significant reduction of St3–73P was observed (Fig. 6*D*). The *in vivo* phosphorylation of the *in vitro* identified GSK-3β phosphorylation site of stathmin 3 being inhibited by well characterized GSK-3β pharmacological inhibitors, it is likely that stathmin 3 is indeed a substrate for GSK-3β in live neurons.

Inhibition of GSK-3β Induces Stathmin 3 Relocalization in Hippocampal Neurons in Culture—The specific subcellular localization of St3–60P in neurons in culture prompted us to ask whether the overall subcellular localization of stathmin 3 is dependent on its phosphorylation level by GSK-3β. To answer this question, we treated hippocampal neurons in culture with the GSK-3β inhibitor AR-A014418. We did observe, as it has been described (37, 46, 52), that GSK-3β inhibition led to abnormal neuronal morphology, with neurons appearing more ramified and less differentiated in the presence of the inhibitor

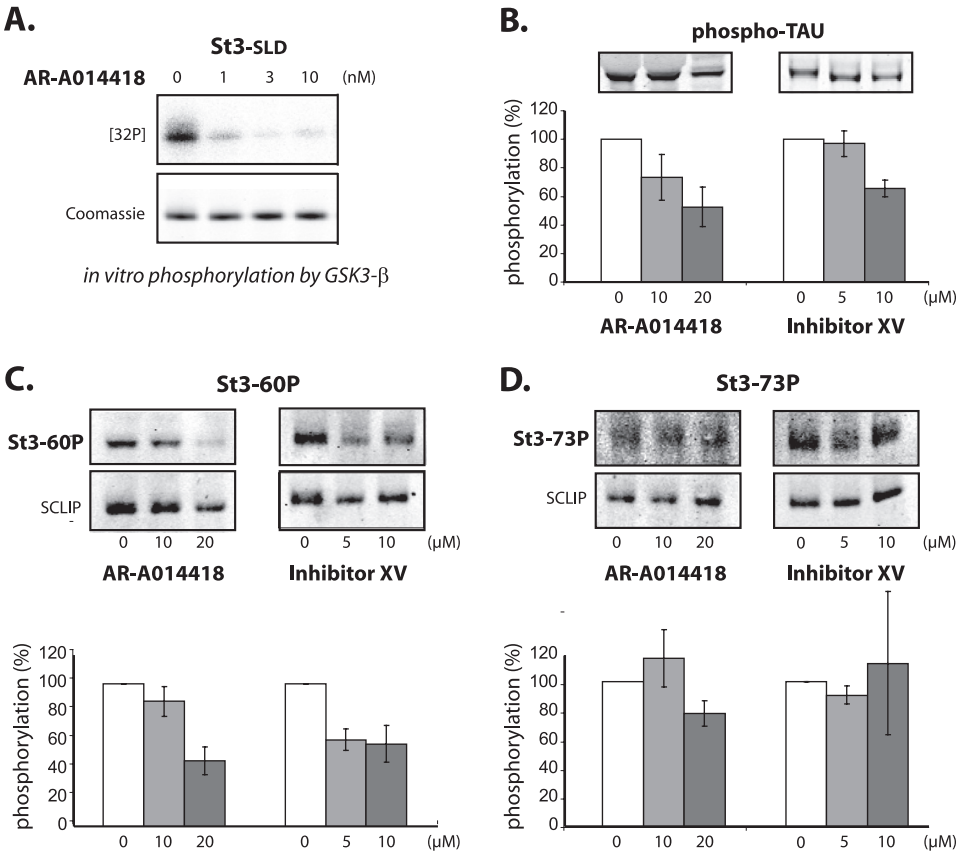

FIGURE 6. **GSK-3β inhibitors specifically inhibit phosphorylation of stathmin 3 at serine 60.** *A*, wild-type St3-SLD recombinant protein was phosphorylated by GSK-3β in the presence of increasing amounts of the GSK-3β inhibitor AR-A014418. Reaction products were analyzed by SDS-PAGE followed by Coomassie Blue staining and phosphorimaging, which reveals the efficacy of the inhibitor on stathmin 3 phosphorylation. *B–D*, hippocampal neurons in culture (2 days *in vitro*) were treated for 24 h with the GSK-3β inhibitor AR-A014418 (10 and 20 μM) or Inhibitor XV (5 and 10 μM). Total cell extracts were separated by SDS-PAGE and analyzed by Western blot with specific antibodies for phospho-Tau (*B*), St3–60P (*C*), and St3–73P (*D*). Quantifications (*bottom panels* in *B–D*) of the respective phospho-specific signal relative to tubulin (*B*) or total stathmin 3 protein (*C* and *D*) performed on at least three different experiments (histograms: mean ± S.E.) confirm the expected efficacy of the GSK-3β inhibitors on phosphorylation of Tau and hence demonstrate their specificity for inhibiting phosphorylation of stathmin 3 on serine 60 in neurons *in vivo*.

at 20 μM (data not shown). Interestingly, the treated cells seemed to also display a modified subcellular stathmin 3 immunoreactivity distribution, in particular as compared with stathmin 2, whose distribution did not seem to be affected. Indeed, in control neurons, both stathmin 2 and 3 were immunodetected as expected at the Golgi, along the neurite shafts, and in neurite tips and growth cones. In contrast, in GSK-3β-inhibited neurons, whereas no significant difference was apparent in stathmin 2 distribution, stathmin 3 appeared somewhat more diffuse and was mainly detected at the Golgi, with a clear decrease and lack of punctuate staining in neurite tips and the growth cone (Fig. 7*A*). To quantify this observation, we performed triple labeling of rat hippocampal neurons with anti-tyrosinated tubulin, anti-stathmin 2 or 3, and anti-Golgi (CTR-433) antibodies. The Golgi and tubulin labelings were used to define "masks" covering either the Golgi area of each cell considered or the entire cell minus the Golgi, respectively. These two masks were used to quantify the mean intensity of stathmin 2 or 3 labeling in the two corresponding areas of each cell. The ratio between the intensity per surface area in the Golgi and the rest of the cells was calculated for at least 20 cells in each condition in three separate experiments (Fig. 7*B*). Quantifications reveal that there was indeed a significant increase of this ratio for stathmin 3 in the treated cells compared with control cells. This effect is dose-dependent and is not observed for stathmin 2. Stathmin 3 localization is thus specifically more restricted to the Golgi in neurons where GSK-3β is inhibited. This observation may support the hypothesis of a specific localization of stathmin 3 depending on its phosphorylation by GSK-3β, although it may also more indirectly result from the pleiotropic actions of GSK-3β during neuronal differentiation.

DISCUSSION

During neuronal differentiation, growth cone progression, neurite elongation, and axonal branching rely on essential cytoskeleton rearrangements. Stathmin family phosphoproteins are involved in the regulation of such developmental processes as they are microtubule regulating proteins highly expressed in the nervous system (2, 5, 13, 53). Although similar in many respects, stathmin 2 (SCG10) and stathmin 3 (SCLIP) fulfill distinct, independent and complementary regulatory roles in axonal morphogenesis (26). We show here for the first time that, in contrast to the other stathmins, stathmin 3 is a specific substrate for GSK-3β, a proline-dependent protein kinase playing prominent roles in neuronal differentiation. We further show that stathmins 2 and 3 possess distinct phosphorylation

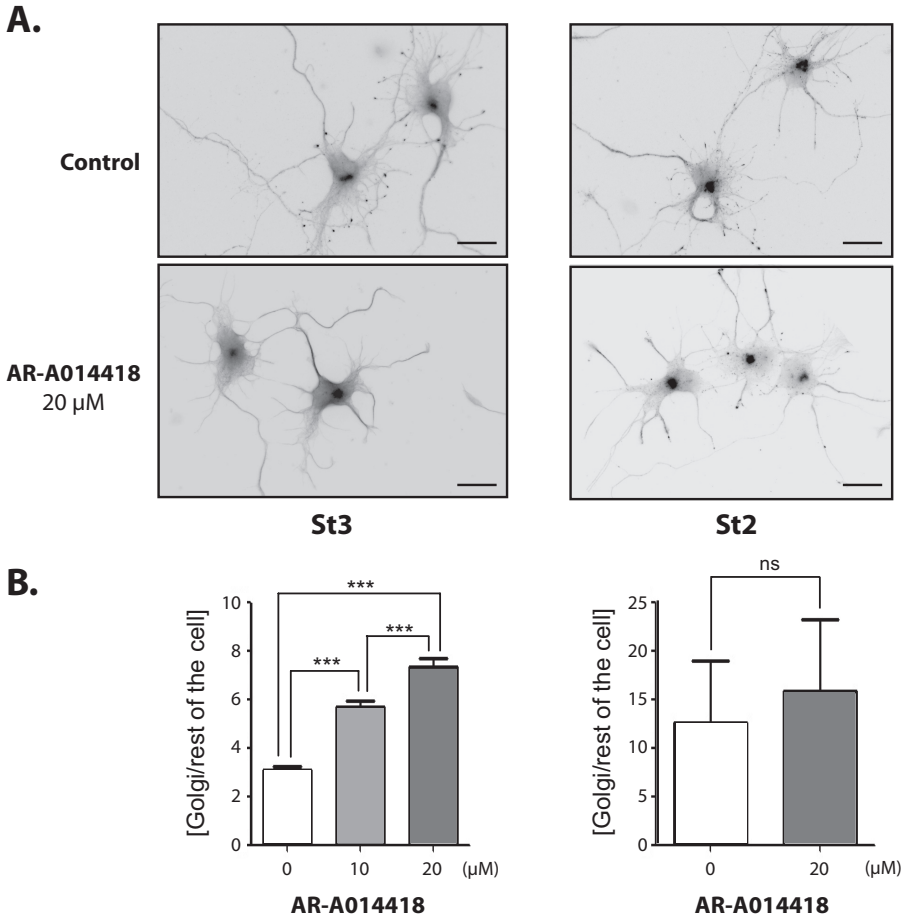

FIGURE 7. **GSK-3β inhibitor induces stathmin 3 relocalization in hippocampal neurons in culture.** Hippocampal neurons in culture (2 *days in vitro*) were treated for 24 h with vehicle (*Control*) or with the GSK-3β inhibitor AR-A014418, and then immunolabeled for stathmin 3 (*St3*) or stathmin 2 (*St2*). *A,* representative images of each condition, showing the redistribution and loss of punctuate labeling of stathmin 3 but not stathmin 2 in the presence of the GSK-3β inhibitor AR-A014418. *Bar* = 20 μm. *B,* quantification of stathmin 3 or stathmin 2 immunoreactivity in the Golgi area relative to the rest of the cell ($n = 20$). Statistical comparisons, using the Mann-Whitney test, show a significant difference between control and treated cells for stathmin 3 labeling (***, $p < 0.0003$) but no significant difference for stathmin 2 ($p > 0.05$). Similar results were obtained in three independent experiments.

sites differentially regulated by proline-directed kinases within their specific proline-rich domains. Finally, we demonstrate the specific localization of stathmin 3 in actin-rich regions at neurite tips when phosphorylated at serine 60 likely by GSK-3β. Stathmin proteins can thus be either regulated locally or locally targeted by specific phosphorylation, which likely participates in their specific roles in neuronal differentiation.

Stathmin 3 Possesses Specific Phosphorylation Sites within Its PRD Region and Is a Target for GSK-3β Both in Vitro and in Vivo—Stathmins display a high degree of sequence identity within their SLDs, with the exception of their 14–16-residue proline-rich PRD region (2, 6). Interestingly, stathmins 2 and 3 did not display homologous patterns of phosphorylation sites for the two classical proline-directed kinases ERK2 and CDK5, both *in vitro* and in transfected cells in culture. In particular, serine 68 of stathmin 3 is a target for ERK2 instead of serine 60 as would be expected by comparison with serine 62 of stathmin 2, whereas serine 60 is the main site for GSK-3β, which does not phosphorylate stathmin 2.

It is interesting to note that the diverging PRD sequence was considered so far as a mere unstructured linker between the two well defined tubulin-interacting regions of stathmins as revealed by x-ray crystallography (16). However, as the PRD region is conserved through evolution within each member of the stathmin family and includes specific proline-serine phosphorylation sites, it is likely that it also fulfills specific and functional regulatory roles. One possibility is that the resulting regulation could apply indirectly on the tubulin interacting properties of the given stathmins. However, phosphorylation of the proline-dependent sites within the PRD of stathmin 1 is not very effective at inhibiting its interaction with tubulin (54). It is thus more likely that phosphorylation within their PRD regulates some other yet unidentified properties of stathmins and/or their interaction with other cellular partners.

The specific phosphorylation of stathmin 3 by GSK-3β is of particular interest in the context of neuronal differentiation, as this proline-directed kinase is known to play a role in the control of axon formation and morphogenesis (reviewed in Refs. 35–39, 46), and to interact with microtubule regulating proteins such as CRMP2 (36), MAP2 (55), MAP1B (56), or Tau (57). The main phosphorylation target of GSK-3β on stathmin 3 is serine 60. This phosphorylation site might be primed by the possible phosphorylation site at position 65, 5 residues downstream as described for some GSK-3β substrates (58), or it may belong to the nonprimed category of GSK-3β sites such as, for example, in MAP1b (59).

As we were able to show that stathmin 3 is indeed phosphorylated on serine 60 and that this phosphorylation is reduced by GSK-3β inhibitors in differentiating neurons in culture, it is very likely that stathmin 3 is a direct substrate for this kinase *in vivo*. GSK-3β is also known to be involved in the phosphorylation of Tau and APP, and to be overactivated in brains of Alzheimer patients (60). It would thus be of interest to examine if the phosphorylation of stathmin 3 at serine 60 is affected in this pathology.

Stathmin 3 Phosphorylated at Serine 60 Is Present at the Growth Cone—We have shown that stathmin 3 phosphorylated at serine 60 (St3–60P) but not stathmin 3 phosphorylated at serine 73 (St3–73P) is located at neurite tips and in particular within the growth cone. It is interesting to note that, by contrast, phosphorylated stathmin 2 is absent from the growth cone of retinal ganglion neurons (61). Moreover, inhibition of GSK-3β, which reduces the phosphorylation level of stathmin 3 at serine 60, induced a relocalization of stathmin 3 toward the cell body in hippocampal neurons in culture. These results suggest that serine 60 phosphorylation of stathmin 3 is important for its specific localization at the leading edge of the cell. Interestingly, a similar DOCK7-mediated phosphorylation-related subcellular localization along the axon was previously described for stathmin 1: in early stage hippocampal neurons, local phosphorylation of stathmin 1 at serine 16 is higher in the nearly formed axon than in the future dendrites, and increases toward the distal edge of growing axons (28). Other microtubule-associated proteins have been shown to have their spatiotemporal localization regulated by phosphorylation, such as for example, doublecortin (DCX) which, like stathmin, possesses a tubulin-binding site and a proline-rich domain (62), or MAP1B whose phosphorylation on nonprimed GSK-3β sites is restricted to growing axons (59).

How St3–60P is selectively localized at neurite tips is presently unknown. One possibility is that stathmin 3 is specifically phosphorylated locally at the growth cone. The overall redistribution of stathmin 3 protein toward the soma upon GSK-3 inhibition could reveal that, conversely, its phosphorylation by GSK-3β would result in the migration of additional stathmin 3 toward neurites and their tips. This migration could either provide more substrate for the kinase or compensate for the unphosphorylated protein that has been phosphorylated locally. Alternatively, stathmin 3 may be partially targeted to the leading edge of neurites upon phosphorylation at serine 60. Such a process has been recently shown for stathmin 1 through its association to a specific kinesin complex when phosphorylated at serine 38 (63, 64).

Stathmin 3 Phosphorylated at Serine 60 Colocalizes with Actin in the Growth Cone Peripheral Domain and Axonal Filopodia—We observed previously the presence of stathmins 2 and 3 along dynamic exploratory microtubules within the actin-rich peripheral zone of the growth cone (26). We show here that stathmin 3 mostly in its serine 60-phosphorylated form colocalizes with the actin-rich structures at neurite extremities, as well as in filopodial extensions along neurites. Although a direct interaction of stathmin 3 with actin has not been demonstrated so far, stathmin 3 could be another protein, regulated by phosphorylation, contributing to the interactions between the actin and tubulin networks.

Indeed, neurite outgrowth necessitates coordinated events between the two major cytoskeletal components actin and tubulin (65). This integration could be mediated by molecules such as Pod-1, which contains molecular microtubule and actin-binding domains (66). However, there are also few examples of molecular complexes that can bridge between these cytoskeletal components, such as for example, the Spn-DCX interaction (67), DCX being known to interact with microtubules (68), whereas Spn is able to cross-link F-actin into bundles (69). These two proteins display maximal overlap in the proximal part of the growing neurite tip. Interestingly, DCX colocalization with actin is mediated by phosphorylation by JNK. Under normal activity, DCX invades the actin-rich region of the growth cone, but this invasion decreases when JNK activity is inhibited (62).

In the case of stathmin 3, it could either interact directly with actin, for example, through its PRD region, which does not interact with tubulin, or through another intermediate partner to be identified. It is interesting to note that, although not formally recognized as a stathmin partner at the time, actin from a brain homogenate was retained, like tubulin, on a stathmin affinity column (70). A direct or indirect interaction with actin dynamics could also explain the previously described involvement of stathmin 3 in the control of axonal branching (26), which takes place at the growth cone and along the shaft when microtubules splay apart, allowing shorter microtubules to invade the nascent actin-rich branches (71, 72).

In conclusion, our results provide new insight into the molecular bases and pathways allowing distinct and specific functions and regulation of phosphoproteins of the stathmin family. We showed for the first time that stathmins 2 and 3 are regulated differently by phosphorylation, that stathmin 3 is a unique stathmin substrate for GSK-3β, which phosphorylates it on a site related to its subcellular localization. Such specific, potential local phosphorylation in response to various extracellular or intracellular cues may direct the specific, diverse functions of various members of the stathmin family in neurons. Moreover, phosphorylation of stathmin 3 could contribute also to the integration between the actin and tubulin networks at the dynamic edge of growing neurites. Elucidating these pathways and understanding the molecular mechanisms relating phosphorylation and subcellular localization of stathmins will be of high interest to better understand the process involved in the development and maturation of the nervous system.

Acknowledgments—We thank Dr Alexandre Maucuer for help and many valuable discussions and Dr. Jean-Baptiste Sibarita for advice in imaging approaches. Fluorescence and confocal microscopy was performed in the Institut du Fer à Moulin Imaging facility.

REFERENCES

1. Sobel, A. (1991) Stathmin. A relay phosphoprotein for multiple signal transduction? *Trends Biochem. Sci.* **16,** 301–305
2. Curmi, P. A., Gavet, O., Charbaut, E., Ozon, S., Lachkar-Colmerauer, S., Manceau, V., Siavoshian, S., Maucuer, A., and Sobel, A. (1999) Stathmin and its phosphoprotein family. General properties, biochemical, and func-

tional interaction with tubulin. *Cell Struct. Funct.* **24,** 345–357
3. Sobel, A., Boutterin, M. C., Beretta, L., Chneiweiss, H., Doye, V., and Peyro-Saint-Paul, H. (1989) Intracellular substrates for extracellular signaling. Characterization of a ubiquitous, neuron-enriched phosphoprotein (stathmin). *J. Biol. Chem.* **264,** 3765–3772
4. Maucuer, A., Moreau, J., Méchali, M., and Sobel, A. (1993) Stathmin gene family. Phylogenetic conservation and developmental regulation in *Xenopus*. *J. Biol. Chem.* **268,** 16420–16429
5. Ozon, S., Byk, T., and Sobel, A. (1998) SCLIP. A novel SCG10-like protein of the stathmin family expressed in the nervous system. *J. Neurochem.* **70,** 2386–2396
6. Ozon, S., Maucuer, A., and Sobel, A. (1997) The stathmin family, molecular and biological characterization of novel mammalian proteins expressed in the nervous system. *Eur. J. Biochem.* **248,** 794–806
7. Beretta, L., Dobránsky, T., and Sobel, A. (1993) Multiple phosphorylation of stathmin. Identification of four sites phosphorylated in intact cells and *in vitro* by cyclic AMP-dependent protein kinase and p34cdc2. *J. Biol. Chem.* **268,** 20076–20084
8. Daub, H., Gevaert, K., Vandekerckhove, J., Sobel, A., and Hall, A. (2001) Rac/Cdc42 and p65PAK regulate the microtubule-destabilizing protein stathmin through phosphorylation at serine 16. *J. Biol. Chem.* **276,** 1677–1680
9. Leighton, I. A., Curmi, P., Campbell, D. G., Cohen, P., and Sobel, A. (1993) The phosphorylation of stathmin by MAP kinase. *Mol. Cell. Biochem.* **127,** 151–156
10. le Gouvello, S., Manceau, V., and Sobel, A. (1998) Serine 16 of stathmin as a cytosolic target for Ca^{2+}/calmodulin-dependent kinase II after CD2 triggering of human T lymphocytes. *J. Immunol.* **161,** 1113–1122
11. Marklund, U., Larsson, N., Brattsand, G., Osterman, O., Chatila, T. A., and Gullberg, M. (1994) Serine 16 of oncoprotein 18 is a major cytosolic target for the Ca^{2+}/calmodulin-dependent kinase-Gr. *Eur. J. Biochem.* **225,** 53–60
12. Belmont, L. D., and Mitchison, T. J. (1996) Identification of a protein that interacts with tubulin dimers and increases the catastrophe rate of microtubules. *Cell* **84,** 623–631
13. Charbaut, E., Curmi, P. A., Ozon, S., Lachkar, S., Redeker, V., and Sobel, A. (2001) Stathmin family proteins display specific molecular and tubulin binding properties. *J. Biol. Chem.* **276,** 16146–16154
14. Curmi, P. A., Andersen, S. S., Lachkar, S., Gavet, O., Karsenti, E., Knossow, M., and Sobel, A. (1997) The stathmin/tubulin interaction *in vitro*. *J. Biol. Chem.* **272,** 25029–25036
15. Lachkar, S., Lebois, M., Steinmetz, M. O., Guichet, A., Lal, N., Curmi, P. A., Sobel, A., and Ozon, S. (2010) *Drosophila* stathmins bind tubulin heterodimers with high and variable stoichiometries. *J. Biol. Chem.* **285,** 11667–11680
16. Ravelli, R. B., Gigant, B., Curmi, P. A., Jourdain, I., Lachkar, S., Sobel, A., and Knossow, M. (2004) Insight into tubulin regulation from a complex with colchicine and a stathmin-like domain. *Nature* **428,** 198–202
17. Honnappa, S., Jahnke, W., Seelig, J., and Steinmetz, M. O. (2006) Control of intrinsically disordered stathmin by multisite phosphorylation. *J. Biol. Chem.* **281,** 16078–16083
18. Steinmetz, M. O., Jahnke, W., Towbin, H., García-Echeverría, C., Voshol, H., Müller, D., and van Oostrum, J. (2001) Phosphorylation disrupts the central helix in Op18/stathmin and suppresses binding to tubulin. *EMBO Rep.* **2,** 505–510
19. Jourdain, L., Curmi, P., Sobel, A., Pantaloni, D., and Carlier, M. F. (1997) Stathmin. A tubulin-sequestering protein that forms a ternary T2S complex with two tubulin molecules. *Biochemistry* **36,** 10817–10821
20. Poulain, F. E., and Sobel, A. (2010) The microtubule network and neuronal morphogenesis. Dynamic and coordinated orchestration through multiple players. *Mol. Cell Neurosci.* **43,** 15–32
21. Charbaut, E., Chauvin, S., Enslen, H., Zamaroczy, S., and Sobel, A. (2005) Two separate motifs cooperate to target stathmin-related proteins to the Golgi complex. *J. Cell Sci.* **118,** 2313–2323
22. Chauvin, S., Poulain, F. E., Ozon, S., and Sobel, A. (2008) Palmitoylation of stathmin family proteins domain A controls Golgi *versus* mitochondrial subcellular targeting. *Biol. Cell* **100,** 577–589
23. Di Paolo, G., Lutjens, R., Osen-Sand, A., Sobel, A., Catsicas, S., and Grenningloh, G. (1997) Differential distribution of stathmin and SCG10 in developing neurons in culture. *J. Neurosci. Res.* **50,** 1000–1009
24. Levy, A. D., Devignot, V., Fukata, Y., Fukata, M., Sobel, A., and Chauvin, S. (2011) Subcellular Golgi localization of stathmin family proteins is promoted by a specific set of DHHC palmitoyl transferases. *Mol. Biol. Cell* **22,** 1930–1942
25. Gavet, O., El Messari, S., Ozon, S., and Sobel, A. (2002) Regulation and subcellular localization of the microtubule-destabilizing stathmin family phosphoproteins in cortical neurons. *J. Neurosci. Res.* **68,** 535–550
26. Poulain, F. E., and Sobel, A. (2007) The "SCG10-LIke Protein" SCLIP is a novel regulator of axonal branching in hippocampal neurons, unlike SCG10. *Mol. Cell. Neurosci.* **34,** 137–146
27. Poulain, F. E., Chauvin, S., Wehrlé, R., Desclaux, M., Mallet, J., Vodjdani, G., Dusart, I., and Sobel, A. (2008) SCLIP is crucial for the formation and development of the Purkinje cell dendritic arbor. *J. Neurosci.* **28,** 7387–7398
28. Watabe-Uchida, M., John, K. A., Janas, J. A., Newey, S. E., and Van Aelst, L. (2006) The Rac activator DOCK7 regulates neuronal polarity through local phosphorylation of stathmin/Op18. *Neuron* **51,** 727–739
29. Ohkawa, N., Fujitani, K., Tokunaga, E., Furuya, S., and Inokuchi, K. (2007) The microtubule destabilizer stathmin mediates the development of dendritic arbors in neuronal cells. *J. Cell Sci.* **120,** 1447–1456
30. Grenningloh, G., Soehrman, S., Bondallaz, P., Ruchti, E., and Cadas, H. (2004) Role of the microtubule destabilizing proteins SCG10 and stathmin in neuronal growth. *J. Neurobiol.* **58,** 60–69
31. Ozon, S., El Mestikawy, S., and Sobel, A. (1999) Differential, regional, and cellular expression of the stathmin family transcripts in the adult rat brain. *J. Neurosci. Res.* **56,** 553–564
32. Himi, T., Okazaki, T., Wang, H., McNeill, T. H., and Mori, N. (1994) Differential localization of SCG10 and p19/stathmin messenger RNAs in adult rat brain indicates distinct roles for these growth-associated proteins. *Neuroscience* **60,** 907–926
33. Redeker, V., Lachkar, S., Siavoshian, S., Charbaut, E., Rossier, J., Sobel, A., and Curmi, P. A. (2000) Probing the native structure of stathmin and its interaction domains with tubulin. Combined use of limited proteolysis, size exclusion chromatography, and mass spectrometry. *J. Biol. Chem.* **275,** 6841–6849
34. Antonsson, B., Kassel, D. B., Di Paolo, G., Lutjens, R., Riederer, B. M., and Grenningloh, G. (1998) Identification of *in vitro* phosphorylation sites in the growth cone protein SCG10. Effect of phosphorylation site mutants on microtubule-destabilizing activity. *J. Biol. Chem.* **273,** 8439–8446
35. Jiang, H., Guo, W., Liang, X., and Rao, Y. (2005) Both the establishment and the maintenance of neuronal polarity require active mechanisms. Critical roles of GSK-3β and its upstream regulators. *Cell* **120,** 123–135
36. Yoshimura, T., Kawano, Y., Arimura, N., Kawabata, S., Kikuchi, A., and Kaibuchi, K. (2005) GSK-3β regulates phosphorylation of CRMP-2 and neuronal polarity. *Cell* **120,** 137–149
37. Garrido, J. J., Simón, D., Varea, O., and Wandosell, F. (2007) GSK-3α and GSK-3β are necessary for axon formation. *FEBS Lett.* **581,** 1579–1586
38. Goold, R. G., and Gordon-Weeks, P. R. (2004) Glycogen synthase kinase 3β and the regulation of axon growth. *Biochem. Soc. Trans.* **32,** 809–811
39. Kim, Y. T., Hur, E. M., Snider, W. D., and Zhou, F. Q. (2011) Role of GSK-3 signaling in neuronal morphogenesis. *Front. Mol. Neurosci.* **4, article 48,** 1–11
40. Gavet, O., Ozon, S., Manceau, V., Lawler, S., Curmi, P., and Sobel, A. (1998) The stathmin phosphoprotein family. Intracellular localization and effects on the microtubule network. *J. Cell Sci.* **111,** 3333–3346
41. Goslin, K., Assmussen, H., and Banker, G. (1998) in *Culturing Nerve Cells* (Banker G., and K. Goslin, K., eds) pp. 339–370, MIT Press, Cambridge, MA
42. Koppel, J., Boutterin, M. C., Doye, V., Peyro-Saint-Paul, H., and Sobel, A. (1990) Developmental tissue expression and phylogenetic conservation of stathmin, a phosphoprotein associated with cell regulations. *J. Biol. Chem.* **265,** 3703–3707
43. Gupta, A., and Tsai, L. H. (2003) Cyclin-dependent kinase 5 and neuronal migration in the neocortex. *Neurosignals* **12,** 173–179
44. Fukunaga, K., and Miyamoto, E. (1998) Role of MAP kinase in neurons. *Mol. Neurobiol.* **16,** 79–95

45. Hayashi, K., Pan, Y., Shu, H., Ohshima, T., Kansy, J. W., White, C. L., 3rd, Tamminga, C. A., Sobel, A., Curmi, P. A., Mikoshiba, K., and Bibb, J. A. (2006) Phosphorylation of the tubulin-binding protein, stathmin, by Cdk5 and MAP kinases in the brain. *J. Neurochem.* **99,** 237–250
46. Kim, W. Y., Wang, X., Wu, Y., Doble, B. W., Patel, S., Woodgett, J. R., and Snider, W. D. (2009) GSK-3 is a master regulator of neural progenitor homeostasis. *Nat. Neurosci.* **12,** 1390–1397
47. Dotti, C. G., Sullivan, C. A., and Banker, G. A. (1988) The establishment of polarity by hippocampal neurons in culture. *J. Neurosci.* **8,** 1454–1468
48. Dent, E. W., and Gertler, F. B. (2003) Cytoskeletal dynamics and transport in growth cone motility and axon guidance. *Neuron* **40,** 209–227
49. Bhat, R., Xue, Y., Berg, S., Hellberg, S., Ormö, M., Nilsson, Y., Radesäter, A. C., Jerning, E., Markgren, P. O., Borgegård, T., Nylöf, M., Giménez-Cassina, A., Hernández, F., Lucas, J. J., Díaz-Nido, J., and Avila, J. (2003) Structural insights and biological effects of glycogen synthase kinase 3-specific inhibitor AR-A014418. *J. Biol. Chem.* **278,** 45937–45945
50. Atilla-Gokcumen, G. E., Williams, D. S., Bregman, H., Pagano, N., and Meggers, E. (2006) Organometallic compounds with biological activity. A very selective and highly potent cellular inhibitor for glycogen synthase kinase 3. *Chembiochem.* **7,** 1443–1450
51. Hanger, D. P., and Noble, W. (2011) Functional implications of glycogen synthase kinase-3-mediated Tau phosphorylation. *Int. J. Alzheimers Dis.* **2011,** 352805
52. Shi, S. H., Cheng, T., Jan, L. Y., and Jan, Y. N. (2004) APC and GSK-3β are involved in mPar3 targeting to the nascent axon and establishment of neuronal polarity. *Curr. Biol.* **14,** 2025–2032
53. Riederer, B. M., Pellier, V., Antonsson, B., Di Paolo, G., Stimpson, S. A., Lütjens, R., Catsicas, S., and Grenningloh, G. (1997) Regulation of microtubule dynamics by the neuronal growth-associated protein SCG10. *Proc. Natl. Acad. Sci. U.S.A.* **94,** 741–745
54. Larsson, N., Marklund, U., Gradin, H. M., Brattsand, G., and Gullberg, M. (1997) Control of microtubule dynamics by oncoprotein 18. Dissection of the regulatory role of multisite phosphorylation during mitosis. *Mol. Cell. Biol.* **17,** 5530–5539
55. Sanchez, I., and Cohen, W. D. (1994) Assembly and bundling of marginal band microtubule protein. Role of Tau. *Cell Motil. Cytoskeleton* **29,** 57–71
56. Geraldo, S., and Gordon-Weeks, P. R. (2009) Cytoskeletal dynamics in growth-cone steering. *J. Cell Sci.* **122,** 3595–3604
57. Hanger, D. P., Anderton, B. H., and Noble, W. (2009) Tau phosphorylation. The therapeutic challenge for neurodegenerative disease. *Trends Mol. Med.* **15,** 112–119
58. Soutar, M. P., Kim, W. Y., Williamson, R., Peggie, M., Hastie, C. J., McLauchlan, H., Snider, W. D., Gordon-Weeks, P. R., and Sutherland, C. (2010) Evidence that glycogen synthase kinase-3 isoforms have distinct substrate preference in the brain. *J. Neurochem.* **115,** 974–983
59. Scales, T. M., Lin, S., Kraus, M., Goold, R. G., and Gordon-Weeks, P. R. (2009) Nonprimed and DYRK1A-primed GSK-3β phosphorylation sites on MAP1B regulate microtubule dynamics in growing axons. *J. Cell Sci.* **122,** 2424–2435
60. Kremer, A., Louis, J. V., Jaworski, T., and Van Leuven, F. (2011) GSK-3 and Alzheimer disease. Facts and fiction. *Front. Mol. Neurosci.* **4,** 17
61. Suh, L. H., Oster, S. F., Soehrman, S. S., Grenningloh, G., and Sretavan, D. W. (2004) L1/laminin modulation of growth cone response to EphB triggers growth pauses and regulates the microtubule destabilizing protein SCG10. *J. Neurosci.* **24,** 1976–1986
62. Gdalyahu, A., Ghosh, I., Levy, T., Sapir, T., Sapoznik, S., Fishler, Y., Azoulai, D., and Reiner, O. (2004) DCX, a new mediator of the JNK pathway. *EMBO J.* **23,** 823–832
63. Takahashi, K., and Suzuki, K. (2009) Membrane transport of WAVE2 and lamellipodia formation require Pak1 that mediates phosphorylation and recruitment of stathmin/Op18 to Pak1-WAVE2-kinesin complex. *Cell Signal* **21,** 695–703
64. Takahashi, K., Tanaka, T., and Suzuki, K. (2010) Directional control of WAVE2 membrane targeting by EB1 and phosphatidylinositol 3,4,5-triphosphate. *Cell Signal.* **22,** 510–518
65. Dehmelt, L., and Halpain, S. (2004) Actin and microtubules in neurite initiation. Are MAPs the missing link? *J. Neurobiol.* **58,** 18–33
66. Rothenberg, M. E., Rogers, S. L., Vale, R. D., Jan, L. Y., and Jan, Y. N. (2003) *Drosophila* pod-1 cross-links both actin and microtubules and controls the targeting of axons. *Neuron* **39,** 779–791
67. Bielas, S. L., Serneo, F. F., Chechlacz, M., Deerinck, T. J., Perkins, G. A., Allen, P. B., Ellisman, M. H., and Gleeson, J. G. (2007) Spinophilin facilitates dephosphorylation of doublecortin by PP1 to mediate microtubule bundling at the axonal wrist. *Cell* **129,** 579–591
68. Taylor, K. R., Holzer, A. K., Bazan, J. F., Walsh, C. A., and Gleeson, J. G. (2000) Patient mutations in doublecortin define a repeated tubulin-binding domain. *J. Biol. Chem.* **275,** 34442–34450
69. Satoh, A., Nakanishi, H., Obaishi, H., Wada, M., Takahashi, K., Satoh, K., Hirao, K., Nishioka, H., Hata, Y., Mizoguchi, A., and Takai, Y. (1998) Neurabin-II/spinophilin. An actin filament-binding protein with one pdz domain localized at cadherin-based cell-cell adhesion sites. *J. Biol. Chem.* **273,** 3470–3475
70. Manceau, V., Gavet, O., Curmi, P., and Sobel, A. (1999) Stathmin interaction with HSC70 family proteins. *Electrophoresis* **20,** 409–417
71. Kalil, K., Szebenyi, G., and Dent, E. W. (2000) Common mechanisms underlying growth cone guidance and axon branching. *J. Neurobiol.* **44,** 145–158
72. Szebenyi, G., Callaway, J. L., Dent, E. W., and Kalil, K. (1998) Interstitial branches develop from active regions of the axon demarcated by the primary growth cone during pausing behaviors. *J. Neurosci.* **18,** 7930–7940